Reaction Kinetics and Catalysis Letters 87 (2006) 235-247

Surface and structural properties of Pt/CeO_2 catalyst under preferential CO oxidation in hydrogen (PROX)

D. Teschner[1,2], A.Wootsch[2], O. Pozdnyakova[2], J. H. Sauer[1], A. Knop-Gericke[1], R. Schlögl[1]

[1]Department of Inorganic Chemistry, Fritz-Haber-Institute of the MPG, Faradayweg 4-6, 14195 Berlin, Germany
[2]Institute of Isotopes, CRC, HAS, Budapest, Konkoly-Thege M. 29-33, H-1525, Hungary

* Corresponding author: e-mail teschner@fhi-berlin.mpg.de, phone +49 30 8413 5408, fax +49 30 8413 4676

Abstract

Preferential oxidation of CO in the presence of excess hydrogen was studied on Pt/CeO_2 with 5% metal loading. Catalytic data were similar to those observed on 1% Pt/CeO_2 earlier [Wootsch et al. J. Catal. 225 (2004) 259]. The optimum temperature region is T≤373 K; conversion and selectivity of CO oxidation strongly decreased at higher temperatures. High-pressure XPS indicated CO adsorbed on platinum particles and significant amount of water on the ceria surface. The top-most ceria surface re-oxidized as small amount of oxygen (3%) was introduced into the H_2/CO feed. Despite this surface re-oxidation, high-resolution TEM after reaction indicated oxygen deficient ceria bulk structure, in which the defects formed a super-cell, with $CeO_{1.695}$ structure. The defective ceria is suggested to play an important role stabilizing the hydrogen bonded surface water, which (i) suppresses further hydrogen oxidation and (ii) reacts at the metal/support interface with linearly adsorbed CO in a low temperature water-gas-shift type reaction to produce CO_2.

Keywords: Hydrogen purification, preferential CO oxidation, PROX, platinum, Pt/CeO_2, ceria, high pressure XPS, HRTEM

Introduction

Noble metals dispersed on ceria containing oxide supports represent a special class of supported catalyst [1]. Their particular behavior was demonstrated in various reactions, mainly in oxidations [2,3] but also in reaction of hydrocarbons under reducing environment[4,5]. The irregular properties of noble metal-ceria systems were attributed to the reducibility of ceria support, which can (i) supply extra oxygen to the metallic site by back spillover process [2,4], (ii) may cause increased hydrogen spillover when it is present in the reaction mixture [4,5] and (iii) induce electronic and/or structural changes of metal particles by strong metal-support interaction (SMSI) [6].

In the current paper surface state and structural response of a Pt/ceria catalyst is examined in the PROX reaction, the preferential oxidation of CO in the presence of hydrogen. This reaction is practically important to eliminate traces of carbon monoxide from hydrogen feed to Proton Exchange Membrane Fuel Cell (PEMFC). For its proper operation the CO concentration must be kept under 1-100 ppm, depending on the type of anode [7]. Hydrogen is usually produced by steam reforming (STR), autothermal reforming (ATR) or partial oxidation (POX) of natural gas, light oil fractions or (bio)alcohols [8.9]. Unfortunately, noticeable amount of CO, ca. 5-15%, is formed together with H_2, H_2O and CO_2. A subsequent water gas shift (WGS) reaction can only reduce the amount of CO to 0.5-1% [8]. This high amount of CO can be removed by *pr*eferential *ox*idation (PROX) using mainly Pt or Au nanoparticles supported on reducible oxides (CeOx / FeOx) or using bimetallic catalysts like Pt-Ru, Pt-Sn [10-18]. The difficulty to overcome is to selectively oxidize CO in a very high excess of hydrogen with ideally as little oxygen as possible. The interesting point on these materials is that they show high selectivity towards CO oxidation and optimal performance at temperature on which the fuel cell operates, therefore providing the possibility of implementing the catalyst directly into the fuel cell and make system integration possible for mobile applications.

In the case of platinum/ceria CO can be adsorbed on both platinum and ceria sites, nevertheless the surface coverage of CO on the metallic particles is supposed to be so high that oxygen cannot adsorb on Pt [16,19,20]. Therefore CO oxidation should theoretically perform either on support sites, or after a diffusion/spillover process of one of the reactants on the interface site at the perimeter. However, our combined in-situ DRIFTS, in-situ XPS, HRTEM and TDS study recently suggested somewhat different mechanism [19] as hydrogen-bonded, surface water adsorbed on ceria was proposed to be involved in the reaction. This water can react in a low-temperature water-gas-shift (LTWGS) type reaction with linearly bonded CO at the Pt/ceria interface, forming CO_2 and hydrogen.

In this paper, we aim to understand the morphological changes occurring during PROX reaction on a Pt/ceria sample by correlating catalytic results with in situ XPS study and detailed HRTEM analysis of the ceria phase formed in the reaction.

Experimental

5% Pt/CeO_2 catalyst was prepared by wet impregnation of ceria (Rhodia, 96 m^2 g^{-1}) with aqueous solution of $Pt(NH_3)_4(OH)_2$. The impregnated sample was dried at 393 K overnight and calcined for 4 hours at 773 K in flowing air (30 mL/min) and reduced at 673 K for 4 hours in flowing H_2 (30 mL/min). Dispersion determined by low temperature H_2 adsorption was 18% [21].

Catalytic tests were carried out in an atmospheric continuous flow glass-reactor system. Inlet gases (hydrogen, oxygen and CO) were controlled by mass-flow controllers. Product analysis was preformed by (i) a gas-chromatograph (TCD) equipped with a polar column, Poropak Q, to separate CO_2 and H_2O from the other effluent gases, and (ii) by a hydrogen compensated flue-gas analyzer (MRU DELTA 65-3) for CO and O_2 quantification. Only CO_2 and H_2O were detected as products; methane formation was not observed in our experimental conditions. The total gas inlet was 100 NmL/min, containing 1% CO, 0.5/1% O_2 (oxygen excess, λ, 1 and 2) and rest H_2. Catalysts were activated in situ in flowing air (30 mL/min) at 573 K, before catalytic tests.

In-situ, "high-pressure" XPS experiments were performed at beam line U49/2-PGM2 at BESSY in Berlin. Details about the setup and method were published previously [22,23,24]. A pressed pellet containing about 100 mg of 5%Pt/CeO_2 catalyst was placed on a temperature-controlled heater, and was then activated in-situ in oxygen (0.5 mbar, 573 K). Gas flow (~20 NmL/min) into the reaction cell was controlled using mass flow controllers and leak valves. The PROX mixture contained 0.48 mbar H_2, 0.032 mbar CO and 0.015 mbar O_2. Gas phase analysis was carried out using a quadrupole Balzers mass spectrometer connected through a leak valve to the experimental cell. Ce 3d, O 1s, Pt 4f spectra were recorded with photon energies of hν = 1035, 670 and 260 eV respectively. The binding energies were calibrated using internal references, such as the Ce 3d V (882.4 eV) and U''' (916.7 eV) hybridization states [25] or the Ce 4f state in the band gap. The energy calibration was necessary because surface charging occurred due to the emission of photoelectrons. However, in the PROX mixture, it was only 1-3 eV. Decomposition of the Pt 4f and O 1s regions were performed using Gauss-Lorentz curves, except the metallic Pt 4f component at 71 (and at 74.3) eV that was fitted using Gauss-Lorentz profiles with exponential tail.

HRTEM investigations were performed in a Philips CM200 FEG electron microscope operated at 200 keV. The microscope was equipped with a Gatan imaging filter (GIF 100) and a Gatan Slow-Scan-Camera. The sample was prepared from a piece of catalyst that was activated in O_2 and treated in PROX reaction mixture in the in-situ XPS cell, under conditions analogous to in-situ XPS experiments (see above). HRTEM measurements were carried out on the pure activated sample, as well.

Results and discussion

Catalytic reaction

Figure 1 shows the catalytic pattern of 5% Pt/CeO_2 at atmospheric conditions in the PROX mixture. The oxygen conversion was very high (around 98-100%), while CO conversion decreased as a function of temperature [16]. Almost all CO was converted to CO_2 below 350 K, while oxygen was consumed more and more for the production of water with increasing temperature. Nevertheless, the natural selectivity of Pt towards CO oxidation as opposed to H_2 oxidation manifested itself as lower λ values resulted in higher selectivity (Figure 1b).

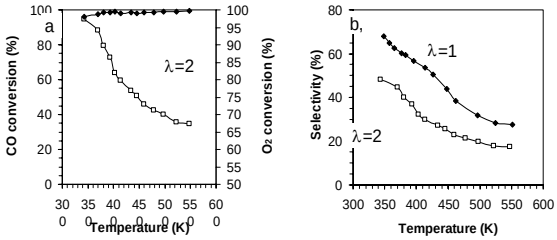

Figure 1: (**a**): CO and O_2 conversion in the PROX mixture at p=1 bar at oxygen excess, λ=2, and (**b**): selectivity towards CO oxidation in the PROX reaction at two λ values.

The catalytic data observed at ~ 0.5 mbar in the in-situ XPS cell are depicted in Figure 2. The activity pattern showed similar trends as at 1 bar, but with slightly different actual values. Increasing temperature decreased the activity and selectivity towards CO oxidation. The much lower conversion in the in-situ XPS cell can be explained by the high dead volume of the setup, i.e. little contact of the gas mixture and the catalyst. In the XPS cell, the 10 mm diameter pellet was placed in a chamber with ca. 8 liters and the total pressure was only 0.5 mbar, while the catalytic flow reactor operated at atmospheric pressure.

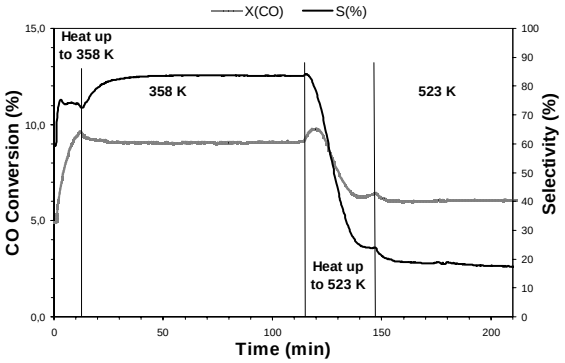

Figure 2: CO conversion and selectivity in the PROX mixture at 0.5 mbar in the in-situ XPS setup.

High pressure XPS

The Pt/CeO_2 sample, investigated in our novel high-pressure XPS setup, was first activated in 0.5 mbar O_2 at 573 K. After that it was cooled down in O_2, and at ~340 K oxygen was exchanged to hydrogen (0.48 mbar). As the ambient temperature was reached, first CO (0.032 mbar) and then O_2 (0.015 mbar) was added to the hydrogen.

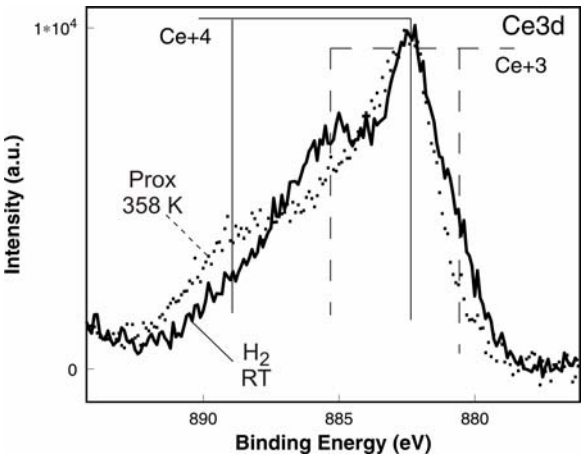

Figure 3: Part of the Ce 3d region of the 5% Pt/CeO_2 at different conditions: in 0.48 mbar H_2 at RT, and in ~ 0.5 mbar PROX mixture at 358 K

Figure 3 depicts part of the Ce3d region recorded in hydrogen (300 K) and in the PROX mixture at 358 K. The surface of ceria was completely oxidized during the activation in oxygen (not shown) while hydrogen induced the formation of Ce^{+3} species. The peaks V and V'' at ~ 882.4 and ~ 888.7 eV, respectively are characteristic for CeO_2, while V^0 and V' (~880.7 and ~885.5 eV) correspond to reduced (Ce^{+3}) ceria [25]. The application of synchrotron radiation as a tunable X-ray source allows us to detect low KE electrons (~140 eV in this part of the spectrum); therefore the information depth of the measurement can be kept small. As in this case, roughly 2-3 ceria layers are probed, mainly the top ceria is reduced in hydrogen. In PROX mixture, however, the surface was clearly re-oxidized. Please note that the mixture contains just 3% oxygen, while all other reactants (~6% CO + ~91% H_2) have a reducing character.

Figure 4a shows the platinum 4f core level (excited with 260 eV photons) in the reaction mixture. The fitting procedure indicated four different components; one is in the zero-valent state, while the others show binding energy shifts of +1-3 eV. As all the high BE components form during the reaction, also when started from a completely reduced state [19], they might not belong to any oxide phase. We identify these peaks as follow: (+1.0 eV component) surface core level shift induced by on-top adsorbed CO [26]; (+1.6 eV component) small Pt clusters or interface Pt atoms in a strong interaction with ceria [19]; (+3.0 eV component, if indeed present) Pt with adsorbed O atoms [27].

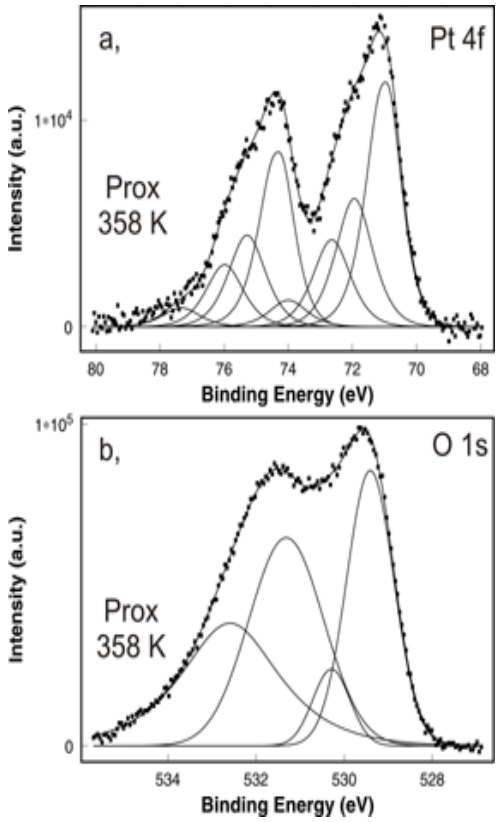

Figure 4: (**a**) Pt 4f and (**b**) O1s region of 5% Pt/CeO_2 in ~ 0.5 mbar PROX mixture at 358 K

In Figure 4b the O 1s spectrum of Pt/ceria is given during the reaction. Depth profiling experiment confirmed that the high-binding-energy part of the O 1s spectrum belongs to surface species [19]. Therefore the peak at 529.4 eV corresponds to oxygen in the ceria lattice (bulk oxygen), in agreement with earlier studies [28,29]. The O-to-Pt atomic ratio was roughly in the range of 100, thus all the resolvable information in the O 1s region should necessarily correspond to ceria. During reaction a strongly pronounced broad peak overlapped with the lattice oxygen component, indicating the presence of OH groups (531.3 eV) on the surface. This peak was asymmetrically broadened to the high energy side, thus lots of water (~532.7 eV) were adsorbed on the ceria surface. Different types of car-

bonates exist on the surface of ceria (see DRIFTS data in [19]) therefore they should be also buried in this part of O 1s. Curve fitting indicated a component at ~ 530.2 eV that can belong to some carbonate species. Obviously they might be also buried under the OH peak, not resolvable from the measurement.

High Resolution Transmission Electron Microscopy (HRTEM)

High resolution TEM measurements were performed on the activated and on the post-reaction Pt/CeO_2 (used in the XPS cell at 0.5 mbar PROX mixture at 358 K). The ceria particles (8-10 nm) were strongly stacked together

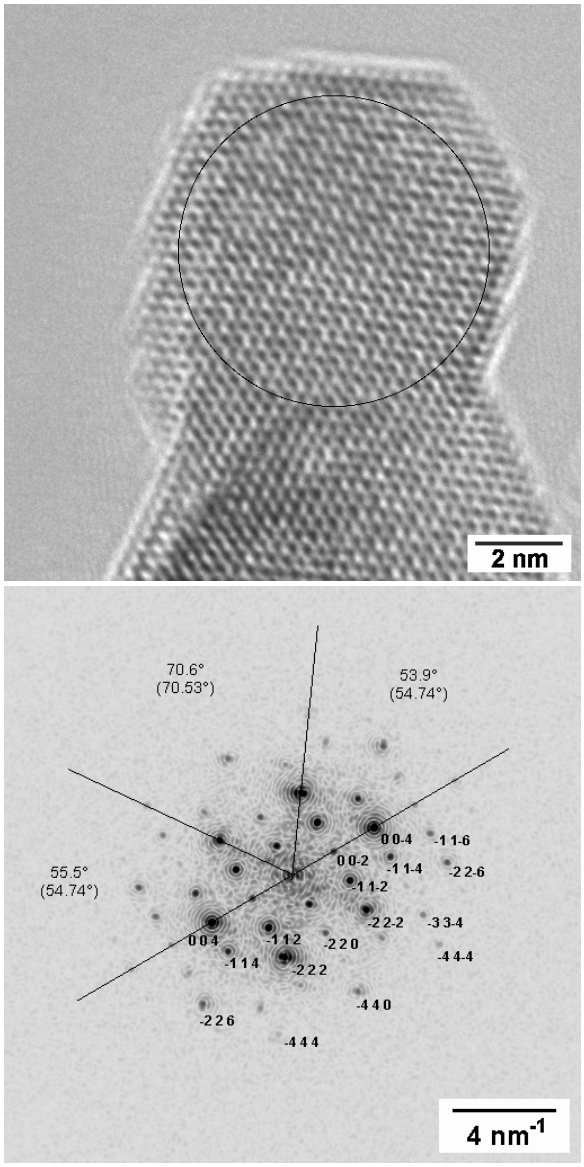

Figure 5: (**a**) High-resolution TEM image of 5% Pt/CeO_2 after PROX reaction at 358 K; (**b**) power spectrum of the selected area indicating reflections not allowed for CeO_2, indexed for $CeO_{1.695}$

Table 1: Measured and reference (CeO_2 and $CeO_{1.695}$) lattice fringes (d)

d (nm)		
Measured	Reference CeO_2	Reference $CeO_{1.695}$
0.7727	–	0.7857 (-110)
0.3923	–	0.3928 (-220)
0.1954	0.1913 (-220)	0.1964 (-440)
0.5474	–	0.5555 (00-2)
0.2757	0.2706 (00-2)	0.2778 (00-4)
0.1851	–	0.1852 (00-6)
0.4533	–	0.4536 (-11-2)
0.4493	–	0.4536 (-112)
0.3173	0.3125 (-11-1)	0.3207 (-22-2)
0.1606	0.1562 (-22-2)	0.1604 (-44-4)
0.3192	0.3125 (-111)	0.3207 (-222)
0.1606	0.1562 (-222)	0.1604 (-444)
0.2629	–	0.2619 (-11-4)
0.2602	–	0.2619 (-114)
0.1912	–	0.1905 (-33-4)
0.1809	–	0.1802 (-11-6)
0.1660	0.1632 (-113)	0.1675 (-226)
0.1676	0.1632 (-11-3)	0.1675 (-22-6)

(despite the cautious sample preparation), thus phase identification was restricted to the minor part of the specimen, where less ceria particles are on top of each other. Platinum particles are mainly of 2-3 nm in diameter, but there are some indications [19] that even few atomic clusters (5-6 Å) are also present in the activated sample. Most of the ceria particles were in form of CeO_2 (fluorite structure) with [111], [110] and [001] orientation. In some cases small lattice expansion and stronger angular distortion could be calculated mainly because some defective structures. After reaction, part of the ceria particles were still in the oxidized CeO_2 state with strong lattice distortion, but part of them were reduced. However, crystalline Ce_2O_3 has never been observed. Figure 5 depicts a typical reduced ceria particle and the power spectrum of the selected part of the image. The power spectrum indicated inverse lattice fringes not allowed in CeO_2 (see also Table 1). Comparison with possible partly reduced ceria phases [30] revealed the presence of [110] oriented $CeO_{1.695}$ (ICSD collection code 88752 [31]), in which the ordering of oxygen vacancies leads to

the formation of a super-cell with lattice constant slightly more than twice of that of CeO_2. $CeO_{1.695}$ has a cubic structure with space group Ia3-. Some of the reflections are indexed in the power spectrum for the $CeO_{1.695}$ phase. Table 1 indicates as well that the deviations of the reference reduced state from the measured reflections are always smaller. Furthermore, power spectrum simulations were carried out using ideal single crystals (CeO_2 and some possible super lattice structures). Figure 6 shows two simple model diffraction patterns (without considering the transmission function of the microscope) for CeO_2 and $CeO_{1.695}$ aligned to each other. It indicates that most of the CeO_2 reflections overlap with that of $CeO_{1.695}$ in such an extent that they are hardly distinguishable. Nevertheless some of them are slightly shifted from each other, which might induce asymmetry of the sum inverse lattice fringes. And indeed, the [-226] spot (indexed for $CeO_{1.695}$) seems to be rather elongated. However other reflections like [-440], [-44-4] and [-22-6] should then be also asymmetric – note they are not – thus the asymmetry of some of the reflections originates from the inhomogeneous angular distortion of ceria in the analysed area rather than from the presence of unreduced CeO_2.

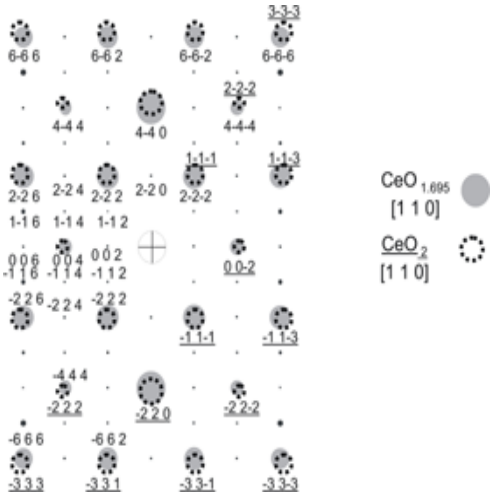

Figure 6: Ideal diffraction patterns for CeO_2 and $CeO_{1.695}$ lattices aligned to each other. Dashed circles and underlined lattice fringes represent CeO_2.

Mechanistic conclusions

Pt/ceria catalysts are very effective materials removing small amount of CO from hydrogen feed gases [13,19]. They show best performance at low temperature (T≤370 K) mainly as water structure in a hydrogen-bonded form is present on the surface of ceria, which according to our previous works [19,20]:

(i.) oxidizes linearly adsorbed CO at the Pt/ceria interface in a low temperature water-gas-shift (LT WGS) type reaction,

(ii.) stabilizes CO at the interface in the linearly bonded state as surface water inhibits the interaction of adsorbed CO with Ce cations, i.e. low amount of "interface-bridging" CO is formed. This bridging-interface CO, formed mainly at higher T, is the precursor for formate species, which was shown to have a negative correlation with the CO_2 production.

(iii.) suppress water formation *on* the platinum particles by shifting the hydrogen oxidation equilibrium back from the reaction.

We have shown that the *surface* of ceria is re-oxidized as CO and O_2 (only 3%) was introduced into the hydrogen feed. This re-oxidation was not complete as revealed by the in-situ XPS spectrum. On the other hand, HRTEM indicated an oxygen deficient super-structure (*bulk*, $CeO_{1.695}$) formed during the reaction.

Defect structures are well studied in widely different topics in the literature. The growth of various metal particles on thin well-ordered oxide films are dominated by defects of the substrate, in which point defects are the primary nucleation centers [32]. Defect structures both in bulk and at the surface have a strong effect also on the adsorptive and catalytic behavior of materials. On TiO_2 (111), for instance, scanning tunneling microscopy gave evidence of oxygen vacancies and their decisive role in the dissociation of water [33]. In the dehydrogenation of ethylbenzene to styrene increasing defect density on α-Fe_2O_3 was found to increase the reaction rate, and the defects were proposed to be the active sites for dehydrogenation [34,35]. Formation of sheer-structure defects were observed by in-situ XRD measurements coinciding with the onset of catalytic activity in propene selective oxidation on molybdenum-oxides [36]. On CeO_2 (111) by using atomic force microscopy, it was established that oxygen vacancies are necessary to adsorb NO_2 and they contribute to the formation of NO_3^- species [37]. Even the oxygen storage capacity (OSC) of ceria was related to its oxygen defect structure [38]. Therefore it is reasonable to assume that the oxygen deficient ceria super-structure observed by HRTEM in our post-reaction sample has a positive effect stabilizing the adsorbed water on its surface. Most probably because of two reasons: (i) increased number of surface OH on such a defective structure that can form H-bonds with adsorbed water, (ii) change in the Ce-Ce surface distance. In fact, prefect CeO_2 does not favor the formation of intermolecular hydrogen bonding networks [39]. Further, it was demonstrated that the reactivity of ceria surface towards water likely depends on the surface termination and morphology [39]. However, as temperature increased, this water structure decomposes, and more and more water desorbs (see TDS in [19]), decreasing the possibility of LT WGS-type reaction. This latter was unequivocally evidenced in Figure 1 and 2, as the yield (and also the selectivity) of CO_2 dramatically decreased as temperature increased.

To sum up, we demonstrated the importance of in-situ techniques like high-pressure XPS, as it reveals surface species and surface oxidation states *during* reaction. Nevertheless, post-reaction methods as HRTEM can also supply

crucial information about phases formed in the reaction (and not decomposed thereafter). The oxygen deficient ceria super-structure seems to stabilize surface water, which is considered in the mechanism of CO oxidation in the presence of hydrogen.

Acknowledgements

D. Teschner and A. Wootsch personally thank to Professor Zoltán Paál for introducing them to the world of heterogeneous catalysis, for his inspiration and valuable advices. A. Wootsch thanks the additional financial support for Grant Bolyai and OTKA Grant no. F046216. In addition, we thank the BESSY staff for their continual support during XPS measurements.

References

[1] A. Trovarelli: *Catal. Rev. Sci. Eng.*, **38,** 439 (1996).
[2] Y. Y. Yung-Fang: *J. Catal*., **87**, 162 (1984).
[3] S. Bedrane, C. Descorme, D. Duprez: *Catal. Today*, **73**, 233 (2002).
[4] D. Teschner, A. Wootsch, T. Röder, K. Matusek, Z. Paál: *Solid State Ionics* **141-142**, 709 (2001).
[5] Z. Paál, A. Wootsch, R. Schlögl, U. Wild: *Appl. Catal. A*, **282**, 135 (2005).
[6] G. L. Haller, D. E. Resasco: *Adv. Catal*., **36**, *173 (1989).*
[7] A. J. Appleby, F. R. Foulkes, Fuel Cell Handbook, Van Nostrand Reinhold, New York, 1989.
[8] J. N. Armor: *Appl. Catal*., **176**, 159 (1999).
[9] F. Aupretre, C. Descorme, D. Duprez: *Catalysis Comm*., **3**, 263 (2002).
[10] G. Avgouropoulos, T. Ioannides, Ch. Papadopoulou, J. Batita, S. Hocevar, H. K. Martalis: *Catal. Today*, **75**, 157 (2002).
[11] G. K. Bethke, H. H. Kung: *Apl. Catal*., **194-195**, 43 (2000).
[12] M. M. Schubert, M. J. Kahlich, H. A. Gasteiger, R. J. Behm: *J. Power Sources*., **84**, 175 (1999).
[13] S. H. Oh, R. M. Sinkevitch: *J. Catal*., **142**, 254 (1993).
[14] M. J. Kahlich, H. A. Gasteiger, R. J. Behm: *J. Catal*., **171**, 93 (1997).
[15] S. Özkara, A. E. Aksoylu: *Appl. Catal. A*, **251**, 75 (2003).
[16] A. Wootsch, C. Descorme, D. Duprez: *J. Catal*., **225**, 259 (2004).
[17] Y.-F. Han, M. J. Kahlich, M. Kinne, R. J. Bhem: *PCCP*., **4**, 389 (2002).
[18] M. M. Schubert, M. J. Kahlich, G. Feldmeyer, M. Hüttner, H. A., Hackensberg, H. A. Gasteiger, R. J. Behm: *PCCP*., **3**, 1123 (2001).
[19] O. Pozdnyakova, D. Teschner, A.Wootsch, J. Kröhnert, B. Steinhauer, H. Sauer, Z. Paál, L. Toth, F. C. Jentoft, A. Knop-Gericke, R. Schlögl: submitted to J. Catalysis (Part I)
[20] O. Pozdnyakova, D. Teschner, A.Wootsch, J. Kröhnert, B. Steinhauer, H. Sauer, Z. Paál, L. Toth, F. C. Jentoft, A. Knop-Gericke, R. Schlögl: submitted to J. Catalysis (Part II)
[21] S. Kacimi, J. Barbier Jr., R. Taha, D. Duprez: *Catal. Lett*. **22**, 343 (1993).
[22] D. F. Ogletree, H. Bluhm, G. Lebedev, C. Fadley, Z. Hussain M. Salmeron: *Rev. Sci. Instrum*., **73**, 3872 (2002).
[23] D. Teschner, A. Pestryakov, E. Kleimenov, M. Hävecker, H. Bluhm, H. Sauer, A. Knop-Gericke, R. Schlögl: *J. Catal*., **230**, 186 (2005).
[24] D. Teschner, A. Pestryakov, E. Kleimenov, M. Hävecker, H. Bluhm, H. Sauer, A. Knop-Gericke, R. Schlögl: *J. Catal*., **230**, 195 (2005).
[25] P. Burroughs, A. Hamnett, A. F. Orchard, G. Thornton: *J. Chem. Soc. Dalton Trans*., **17**, 1686 (1976).
[26] K. Dückers, K. C. Price, H. P. Bonzel, V. Chab, K. Horn: *Phys. Rev. B*., **36**, 6292 (1987).
[27] C.R. Parkinson, M. Walker, C.F. McConville: *Surf. Sci*., **515**, 19 (2003).
[28] D.R. Mullins, S.H. Overbury, D.R. Huntley: *Surf. Sci*., **409**, 307 (1998).
[29] A. Q. Wang, P. Punchaipetch, R. M. Wallace, T. D. Golden: *J. Vac. Sci. Technol. B*, **21**, 1169 (2003).
[30] E. A. Kümmerle, G. Heger: *J. Sol. State Chem.*, **147**, 485 (1999).
[31] http://icsdweb.fiz-karlsruhe.de/
[32] M. Bäumer, M. Frank, M. Heemeier, R. Kühnemuth, S Stempel, H.-J. Freund: *Surf. Sci*., **454-456**, 957 (2000).
[33] R. Schaub, R. Thostrup, N. Lopez, E. Laegsgaard, I, Stensgaard, JK. Norskov, F. Besenbacher: *Phys. Rev. Lett.*, **87**, 266104 (2001).
[34] W. Weiss, D. Zscherpel, R. Schlögl: *Catal. Lett.*, **52**, 215 (1998).
[35] Y. Joseph, M. Wühl, A. Niklewski, W. Ranke, W. Weiss, Ch. Wöll, R. Schlögl: *PCCP*., **2**, 5314 (2000).
[36] T. Ressler, J. Wienold, R. E. Jentoft, T. Neisius: *J. Catal*., **210**, 67 (2002).
[37] Y. Namai, K. Fukui, Y. Iwasawa: *Nanotechnology*, **15**, S49 (2004).
[38] E. Mamontov, T. Egami, R. Brezny, M. Koranne, S. Tyagi: *J. Phys. Chem. B*, **104**, 11110 (2000).
[39] M. A. Hendreson, C. L. Perkins, M. H. Engelhard, S. Thevuthasan, C. H. F. Peden: *Surf. Sci.* **526**, 1 (2003).